The kinetics of CD4+Foxp3+ T cell accumulation during a human cutaneous antigen-specific memory response in vivo

Milica Vukmanovic-Stejic,[1] Elaine Agius,[1,2] Nicola Booth,[1] Padraic J. Dunne,[3] Katie E. Lacy,[1,2] John R. Reed,[1,2] Toni O. Sobande,[1] Steven Kissane,[4] Mike Salmon,[4] Malcolm H. Rustin,[2] and Arne N. Akbar[1]

[1]Department of Immunology, Division of Infection and Immunity, University College London, London, United Kingdom. [2]Department of Dermatology, Royal Free Hospital, London, United Kingdom. [3]Immune Regulation Research Group, School of Biochemistry and Immunology, Biotechnology Building, Trinity College Dublin, Dublin, Ireland. [4]Department of Rheumatology, MRC Centre for Immunoregulation, University of Birmingham, Birmingham, United Kingdom.

Naturally occurring CD4+CD25hiFoxp3+ Tregs (nTregs) are highly proliferative in blood. However, the kinetics of their accumulation and proliferation during a localized antigen-specific T cell response is currently unknown. To explore this, we used a human experimental system whereby tuberculin purified protein derivative (PPD) was injected into the skin and the local T cell response analyzed over time. The numbers of both CD4+Foxp3− (memory) and CD4+Foxp3+ (putative nTreg) T cells increased in parallel, with the 2 populations proliferating at the same relative rate. In contrast to CD4+Foxp3− T cell populations, skin CD4+Foxp3+ T cells expressed typical Treg markers (i.e., they were CD25hi, CD127lo, CD27+, and CD39+) and did not synthesize IL-2 or IFN-γ after restimulation in vitro, indicating that they were not recently activated effector cells. To determine whether CD4+Foxp3+ T cells in skin could be induced from memory CD4+ T cells, we expanded skin-derived memory CD4+ T cells in vitro and anergized them. These cells expressed high levels of CD25 and Foxp3 and suppressed the proliferation of skin-derived responder T cells to PPD challenge. Our data therefore demonstrate that memory and CD4+ Treg populations are regulated in tandem during a secondary antigenic response. Furthermore, it is possible to isolate effector CD4+ T cell populations from inflamed tissues and manipulate them to generate Tregs with the potential to suppress inflammatory responses.

Introduction

Naturally occurring CD4+CD25hiFoxp3+ Tregs (nTregs) can prevent reactivity to both self and non-self antigens (1–4). Although early studies suggested that these cells are generated as a distinct population in the thymus, CD4+CD25hiFoxp3+ Tregs, which are phenotypically and functionally identical to the thymus-derived population, can also be generated after antigen-induced proliferation of CD4+ T cells in peripheral tissues in mice (5, 6). The rapid division of CD4+CD25hiFoxp3+ Tregs that has been shown to occur in vivo in mice (7) and humans (8) may be a mechanism for maintaining nTregs. This has particularly important implications for the lifelong maintenance of human Tregs after thymic involution, since CD4+CD25hiFoxp3+ T cells in humans have limited capacity for extensive self-renewal, due to short telomeres, and lack telomerase activity (8). It is important to consider the possible difference in behavior and characteristics of nTregs in mice and humans, especially given the potential for species-specific differences that might lead to side effects during therapy (9).

The regulation of immunity and pathology by intervention at the Treg axis has been very successful in animal models, where it has been shown that CD4+CD25hiFoxp3+ T cells can be harnessed to prevent autoimmunity (10, 11), inflammatory disease (12), and transplant rejection (13, 14). Conversely, the inhibition or removal of these cells has been shown to increase immune reactivity to tumors (15). This led to the exciting possibility that these cells might be utilized in identical clinical settings in humans, and some clinical trials that influence Treg generation and/or activity are already in progress (reviewed in refs. 11, 16). The balance between responsive T cells and Tregs during an immune response is crucial to maintain controlled immunity and both cell types need to be present for the lifetime of the organism (17). However, little is known about the coordination of activation of both populations during an antigen-specific response in humans in vivo. Moreover, most studies on CD4+CD25hiFoxp3+ T cells in humans have been performed using peripheral blood populations, and apart from a few notable exceptions (18–20), there are very little data on the behavior of these cells at sites of immune responses in vivo. These data are crucial for the development of new strategies for the manipulation of human nTregs for therapeutic purposes.

We previously established an experimental system for investigating the kinetics of human memory T cell proliferation and differentiation during a secondary immune response in vivo by injecting tuberculin PPD into the skin of individuals who were immunized with bacille Calmette-Guérin (BCG) (21, 22). This procedure is also known as the *Mantoux test* (MT). Responding T cells can be isolated at different times from skin suction blisters that are induced over these lesions (21). In addition, skin punch biopsies of the injected site allow histological analysis of the underlying cellular infiltrates. We utilized the MT model to first examine the kinetics at which CD4+Foxp3+ T cells accumulate and proliferate

Nonstandard abbreviations used: BCG, bacille Calmette-Guérin; HSV, herpes simplex virus; MT, Mantoux test; nTregs, naturally occurring CD4+CD25hiFoxp3+ Tregs; PPD, purified protein derivative.

Conflict of interest: The authors have declared that no conflict of interest exists.

Citation for this article: *J. Clin. Invest.* **118**:3639–3650 (2008). doi:10.1172/JCI35834.

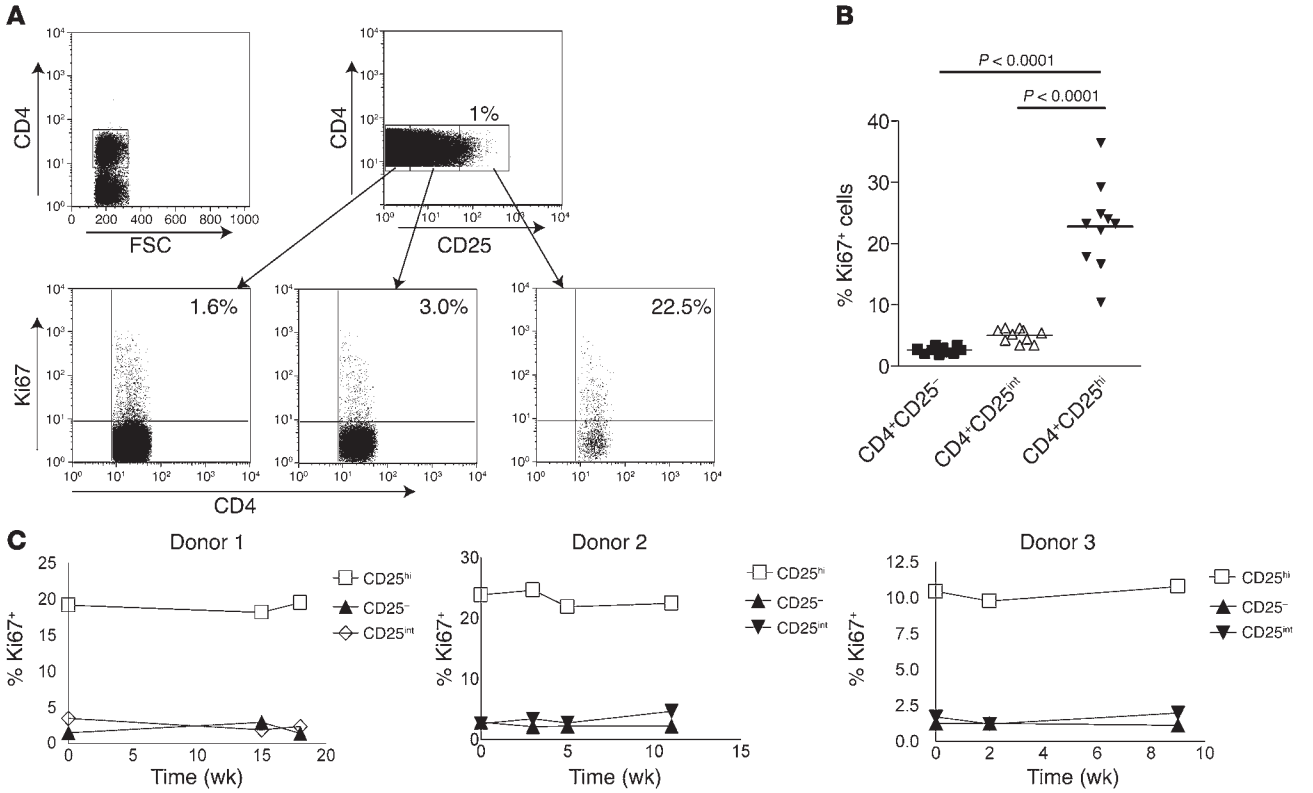

Figure 1
Human CD4+CD25hi Tregs turn over rapidly in vivo. Freshly isolated PBMCs from healthy individuals were stained for CD4/CD25/CD127/Foxp3 and Ki67 following the standard protocol. Tregs were identified as CD25hi, Foxp3+, and CD127lo (for details, see Supplemental Figure 1). (**A**) Expression of Ki67 on CD4+CD25hi, CD4+CD25int, and CD4+CD25− cells from a representative sample. Numbers denote the percentage of cells expressing Ki67 relative to the control gate set with an irrelevant antibody. FSC, forward scatter. (**B**) Cumulative data showing the percentage of Ki67+ cells in each subset. Each symbol represents a different individual (n = 10 per group), and the mean percentage is shown as a horizontal line. Significance was determined by paired t test. (**C**) Graphs show expression of Ki67 in Treg and non-Treg populations examined over the course of 4 months in 3 individuals.

in the skin after antigenic challenge, in relation to memory T cells at the same site. Then we tested the possibility that Tregs can be induced from responsive antigen-specific memory T cells that are isolated from the site of inflammation in vivo.

We show that CD4+Foxp3+ T cells that bear all the phenotypic hallmarks of nTregs accumulate and proliferate at the same relative rate as memory populations in the skin after challenge with recall antigen. A key observation was that human antigen-specific T cells that were isolated from the effector site of these secondary responses in vivo could be converted into anergic, Foxp3-expressing suppressive T cells that had all the hallmarks of the endogenous nTreg pool. It is therefore feasible to isolate, expand, and manipulate pathology-inducing T cell populations from target tissues in vitro in order to generate antigen-specific suppressor T cell populations that may have the potential to suppress inflammatory responses when reintroduced to the host.

Results

Human CD4+CD25hiFoxp3+ Tregs proliferate in vivo. To confirm and extend our previous findings that CD4+CD25+ Tregs are highly proliferative in vivo in humans (8), we analyzed the expression in these cells of Ki67, a nuclear protein expressed by proliferating cells in all phases of the active cell cycle (23). Gating strategy for nTregs was based on high expression of CD25, low expression of CD127, and high expression of Foxp3 (Supplemental Figure 1; supplemental material available online with this article; doi:10.1172/JCI35834DS1). We found that in freshly isolated PBMC populations, in all individuals tested, significantly higher proportions of CD4+CD25+CD127loFoxp3+ T cells expressed Ki67 than CD4+CD25int and CD4+CD25− T cell populations (mean ± SEM, 22.8% ± 2.2% compared with 5% ± 0.3% and 2.6% ± 0.2%, respectively; Figure 1, A and B). This supports previous data showing that human nTregs are highly proliferative in vivo (8). The cycling Foxp3+ Tregs displayed a predominantly CD45RO+ memory phenotype (mean ± SEM, 97% ± 1.2%, n = 10; data not shown). In addition, we followed 3 healthy donors over a period of 3–4 months and observed that the high proliferative activity of nTregs was maintained over time in the absence of any evidence of overt immune activation in vivo (Figure 1C). This raised 2 possibilities that are not mutually exclusive: either thymus-derived nTregs proliferate extensively in the periphery to maintain constant numbers, or proliferating memory T cells are converted to nTregs in the periphery (17). To probe the latter possibility, we first established a human experimental system that enabled us to examine the development, accumulation, and proliferation of CD4+Foxp3+ T cells during a secondary immune response to antigens in vivo.

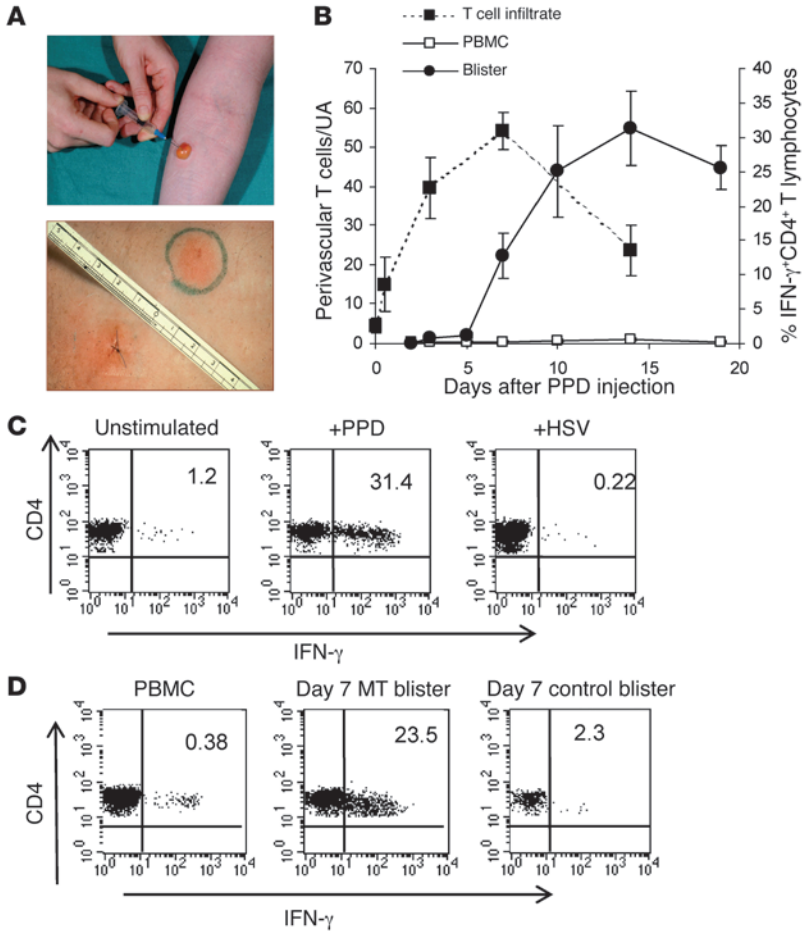

Figure 2
The MT is a well-characterized model of a memory immune response. Samples were collected between 0 and 19 days after PPD injection. (**A**) Skin biopsies were collected for immunohistochemistry (top panel), and cutaneous lymphocytes were isolated from skin suction blisters that were induced over the sites of PPD injection at different time points (lower panel). (**B**) PPD-specific memory T cells accumulate during the course of MT. PBMCs and blister cells were stimulated with PPD for 15 hours in the presence of Brefeldin A and stained for intracellular expression of IFN-γ (right *y* axis, solid lines). The number of $CD3^+$ T cells within dermal perivascular infiltrates was determined by indirect immunoperoxidase staining of 5-μm tissue sections. The 5 largest perivascular infiltrates were counted and data presented per unit area (UA). The mean ± SEM of 5 individuals per time point is shown (dashed line, left *y* axis). (**C**) Blister cells recovered from day 7 blisters were stimulated with PPD or with irrelevant antigen (HSV, CMV, tetanus) or left unstimulated and stained for intracellular expression of IFN-γ. Representative dot plots ($n = 3$ samples per antigen) are shown. Numbers denote the percentage of cells expressing IFN-γ. (**D**) IFN-γ production from day 7 blisters raised over MT response or the site of the control (saline) injection. Numbers denote the percentage of cells expressing IFN-γ. PBMCs and blister cells (PPD and control) from the same donor were stimulated with PPD overnight as described in Methods.

The induction of a memory T cell response in humans in vivo. The MT was induced by the intradermal injection of tuberculin purified protein derivative (PPD) in healthy individuals who had been previously vaccinated against tuberculosis with BCG (Figure 2A). The clinical manifestation of this response is measured by the induction of erythema, induration, and palpability of the lesion (Figure 2A), which peaked at 3 days after PPD injection, as described previously (21, 22). Punch biopsies and skin suction blisters were induced at various time points following the injection of PPD (Figure 2A), permitting the examination of the underlying cellular response. In contrast to clinical response, the infiltrating T cells reached maximal levels 7 days after PPD injection (Figure 2B, dashed line, left axis). $CD4^+$ T cells were the predominant cell type identified in the MT, and 95% of these cells (taken from the lesion) had a $CD45RA^-$ ($CD45RO^+$) $CCR7^{lo}$ phenotype, compared with 50% of $CD4^+$ T cells taken from the same subject's blood (Supplemental Figure 2, A–C). Furthermore, the T cells that accumulated in the skin were highly differentiated, as indicated by low expression of CD45RB (data not shown). Other leukocytes found in the suction blister–derived populations included $CD68^+$ macrophages, $CD1a^+$ Langerhans cells, and $CD11c^+$ and DC-SIGN$^+$ dendritic cells, which have been characterized in this model previously (ref. 21 and data not shown).

We next evaluated the antigen specificity of the skin-infiltrating $CD4^+$ T cells after intradermal challenge. $CD4^+$ T cells harvested from skin suction blisters were assessed for their ability to synthesize IFN-γ after restimulation with PPD in vitro. The proportion of IFN-γ^+ antigen-specific $CD4^+$ T cells increased significantly after PPD injection (Figure 2B; Kruskal-Wallis test, $P < 0.0001$). The proportion of antigen-specific $CD4^+$ T cells detected after antigen challenge on day 14 was considerably higher than that predicted from previous studies that only investigated early time points after injection (0.5%–2.0%) (24). Minimal IFN-γ was synthesized when PPD was not added to the blister cells or when the cells were stimulated with irrelevant antigens such as herpes simplex virus (HSV; Figure 2C), tetanus toxoid, or CMV (data not shown). In contrast, up to 30% of the $CD4^+$ T cells from the skin expressed IFN-γ after PPD restimulation in vitro (Figure 2C). There was no increase in antigen-specific $CD4^+$ T cells in the blood after cutaneous PPD challenge, and the numbers of these cells remained relatively constant at 0.5% of the $CD4^+$ T cell pool at all time points (Figure 2, B and D). In addition, we showed that only 2% of $CD4^+$ T cells that were harvested from a saline control injection at a separate site in the same individual secreted IFN-γ after PPD stimulation (compared with 23% of $CD4^+$ T cells that were isolated from the site of PPD injection) (Figure 2D). There was variability in the size (volume) of blisters from different individuals that was probably related to the physical characteristics of the skin in different subjects. This made the assessment of the absolute numbers of antigen-specific cells unreliable for exact quantitation (range, 500–70,000 IFN-γ^+CD4^+ cells per blister). Therefore, the absolute numbers of PPD-specific cells in the skin is better estimated by

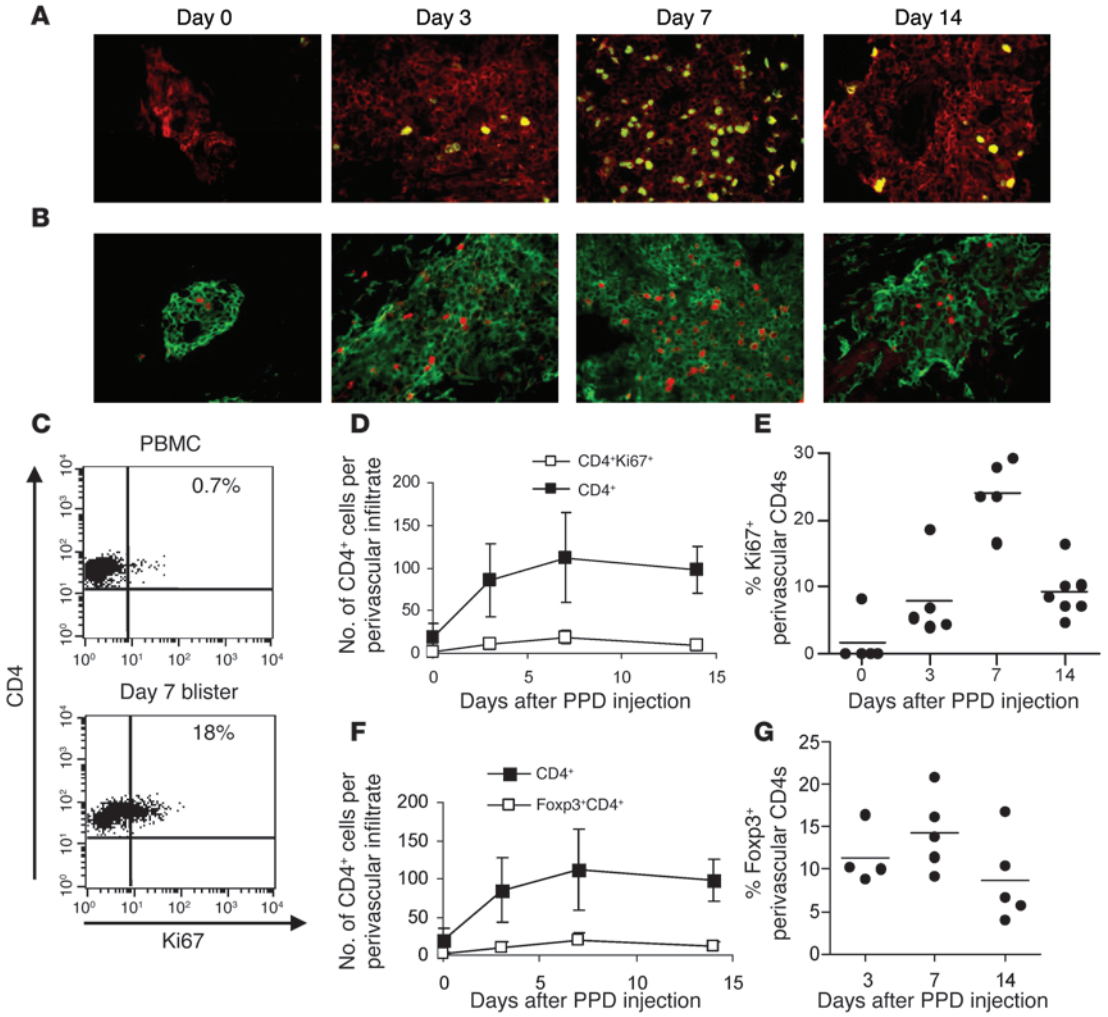

Figure 3

Antigen-specific memory CD4+ T cell proliferation at the site of the MT. (**A**) Double immunofluorescence staining of representative biopsies from days 0, 3, 7, and 14 following MT induction. Green indicates Ki67; red indicates CD4. Original magnification, ×400. (**B**) Double immunofluorescence staining of representative biopsies (days 0, 3, 7, and 14; $n = 5$ per time point) shows CD4+ (green) and Foxp3+ (red) cells in a perivascular lymphocytic infiltrate (original magnification, ×400). The 5 largest perivascular infiltrates present in the upper and middle dermis were selected for analysis. Cell numbers were expressed as the mean absolute number of cells counted within the frame. (**C**) The proportion of Ki67+CD4+ cells was also determined by flow cytometry using blister cells ($n = 3$–5 per time point). Representative dot plots for day 7 PPD blister cells and PBMCs are shown. Numbers denote the percentage of cells expressing Ki67 relative to control gate set with an irrelevant antibody. (**D**) Number of total CD4+ cells (filled squares) and number of Ki67+CD4+ cells (open squares) in perivascular infiltrates following PPD injection. (**E**) Percentage of CD4+ cells expressing Ki67 found per perivascular infiltrate in each donor. Each circle represents an average of 5 perivascular infiltrates counted for each individual ($n = 5$–7 per time point; horizontal lines indicate the mean). (**F**) Number of total CD4+ cells (filled squares) and CD4+Foxp3+ cells (open squares) in perivascular infiltrates following PPD injection. (**G**) Percentage of CD4+ cells expressing Foxp3 per perivascular infiltrate counted. Each symbol represents an average of 5 perivascular infiltrates counted for each individual ($n = 5$–7 per time point). Data are mean ± SEM.

equating together the number of CD4+ T cells in skin sections and the percentage of PPD-specific cells from suction blisters, which was considerably more consistent (Figure 2B). CD8+ antigen-specific T cells in the blisters did not increase during the course of the response and were present at less than 1% at all time-points (data not shown). The MT, therefore, enables the investigation of the kinetics of CD4+ memory T cell accumulation during a secondary immune response in vivo (22).

Accumulation of CD4+Foxp3+ T cells during a secondary response to antigen in vivo. We next investigated whether proliferation of T cells in situ contributed to the accumulation of antigen-specific CD4+ T cells after PPD injection. Tissue biopsies obtained from the site of antigen injection at different times were co-stained with Ki67 and CD4 (Figure 3A). The 5 largest perivascular infiltrates per section were photographed and counted, and data were expressed as mean absolute cell number per frame. Very few proliferating cells were observed in normal skin (day 0), and the perivascular infiltrates were very small or absent. Similar proportions of proliferating CD4+ T cells were identified by flow cytometry of blister (but not PBMC) populations taken at the same time points (Figure 3C and data not shown). At day 7, the time of maximal CD4+ T cell accumulation, the number of CD4+ T cells expressing

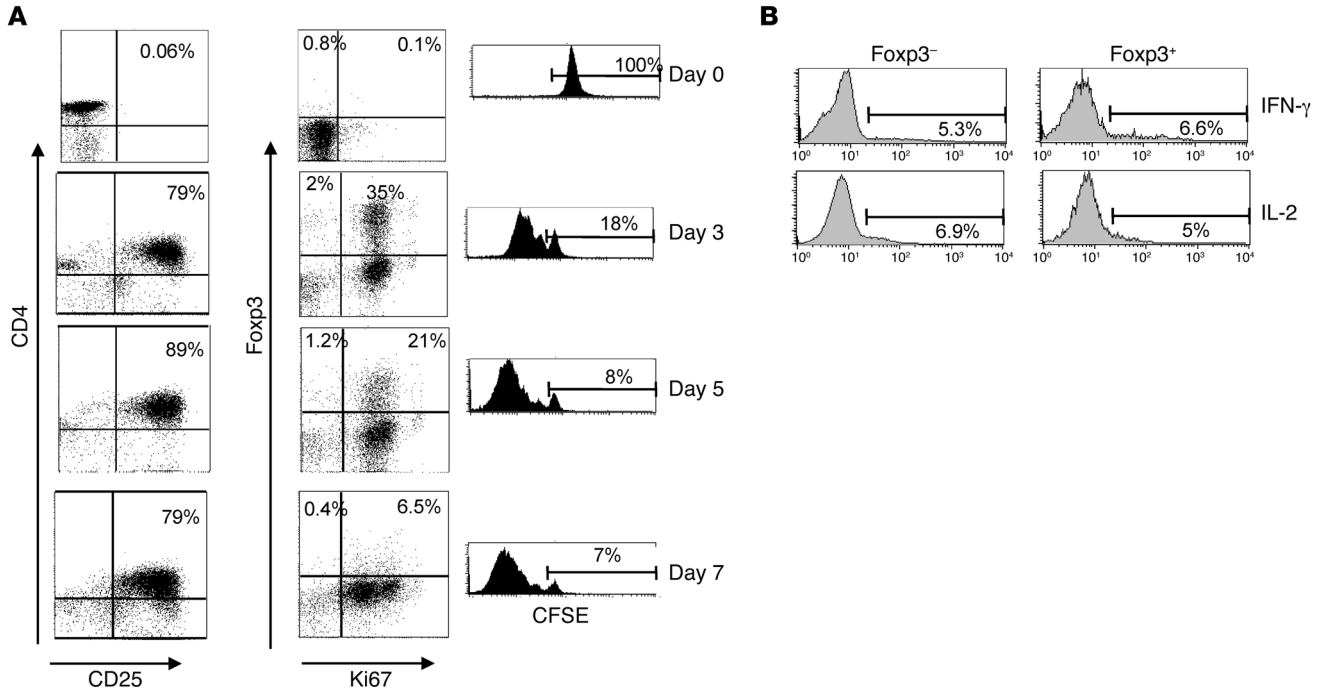

Figure 4

Induction of Foxp3 expression in human CD4⁺CD25⁻ T cells by stimulation. (**A**) CD4⁺CD25⁻ (responder) T cells were isolated from PBMCs using MACS and labeled with CFSE. Cells were stimulated with magnetic beads coated with antibodies to CD3 and CD28 for 7 days. Samples were removed at regular intervals and stained for the expression of CD25, Foxp3, and Ki67. Numbers in dot plots indicate the percentage of cells in each quadrant. Dilution of the CFSE signal indicates proliferation of the cells. Percentages refer to cells that have not divided. Data shown are representative of 3 independent experiments. (**B**) Cells were removed from CD3/CD28-stimulated cultures on day 4 and restimulated with PMA and ionomycin before staining for Foxp3, IL-2, and IFN-γ. Histograms show cytokine production by Foxp3⁻ and Foxp3⁺ cells and are representative of 3 independent experiments. Numbers indicate the percentage of cells expressing IL-2 or IFN-γ.

Ki67 was significantly increased (Figure 3D) and more than 20% of the CD4⁺ T cells were in cycle (Figure 3, A and E). This indicated that the increase in PPD-specific CD4⁺ T cells in the skin after antigenic challenge occurred in part through their extensive local proliferation (Figure 2B).

We have previously shown a high level of proliferation in circulating CD4⁺CD25^{hi} Tregs (8). We examined tissue biopsies taken during MT for the expression of CD4 and Foxp3 and enumerated double-positive cells in the perivascular infiltrates. Figure 3B shows the expression of CD4 and Foxp3 in representative cellular infiltrates at days 0 (control skin), 3, 7, and 14 following PPD injection. Cumulative data from 5 individuals per time point are presented in Figure 3F, showing a significant increase in the number of CD4⁺Foxp3⁺ T cells on day 7 ($P = 0.04$, 1-way ANOVA). This increase in the percentage of CD4⁺Foxp3⁺ cells coincided with the increase in total CD4⁺ T cell numbers and also with peak cellular proliferation ($P = 0.01$, 1-way ANOVA). However, when the corresponding increase in CD4⁺ T cell numbers was taken into account and the data were expressed as the proportion of CD4⁺ T cells expressing Foxp3, this value remained fairly constant during the response (between 8%–15% of CD4⁺ cells; Figure 3G). The percentage of CD4⁺Foxp3⁺ cells on day 0 could not be accurately assessed due to the very low CD4 numbers, although Foxp3⁺ Tregs could be observed in some samples of normal skin (Figure 3B and ref. 25). We concluded that both memory and Foxp3⁺ (putative regulatory) T cells accumulate at the same rate after antigenic stimulation in vivo.

Induction of Foxp3 expression in activated CD4⁺ T cells in vitro. Previous studies have found that human CD4⁺CD25⁻ effector T cells can upregulate Foxp3 transiently, following activation (26–28). It was possible, therefore, that the Foxp3-expressing CD4⁺ T cells that were found in the skin after antigen challenge were activated memory T cell populations that were induced to express this marker temporarily. To clarify this we first investigated the relationship between Foxp3 expression and proliferation in CD4⁺CD25⁻Foxp3⁻ T cells after activation in vitro (Figure 4A). These cells were isolated from peripheral blood, labeled with CFSE, and then activated with anti-CD3/CD28 coated beads. The expression of CD25, Foxp3, and Ki67 was determined on days 0, 3, 5, and 7. By day 3, approximately 80% of cells were CD25⁺ and 35% of CD4⁺ cells expressed Foxp3. All Foxp3⁺ cells were Ki67⁺, and approximately 80% of the activated CD4⁺ T cell population had lost the CFSE label (Figure 4). Most cells lost Foxp3 expression (but remained CD25⁺ and Ki67⁺) by day 7, indicating that the induction of Foxp3 expression in CD4⁺ T cells after activation was transient (Figure 4A).

To assess whether CD4⁺Foxp3⁺ cells that develop as a result of activation exhibit functional characteristics of Tregs, we examined their capacity to synthesize effector cytokines following restimulation, since Tregs do not synthesize IL-2 or IFN-γ (29–32). CD3/CD28-activated CD4 cells were removed from culture on day 4 and restimulated with PMA and ionomycin for 4 hours, followed by staining with Foxp3, IL-2, and IFN-γ (Figure 4B). There was no difference in cytokine production between Foxp3⁺ and Foxp3⁻ cells, indicating that the induction of Foxp3

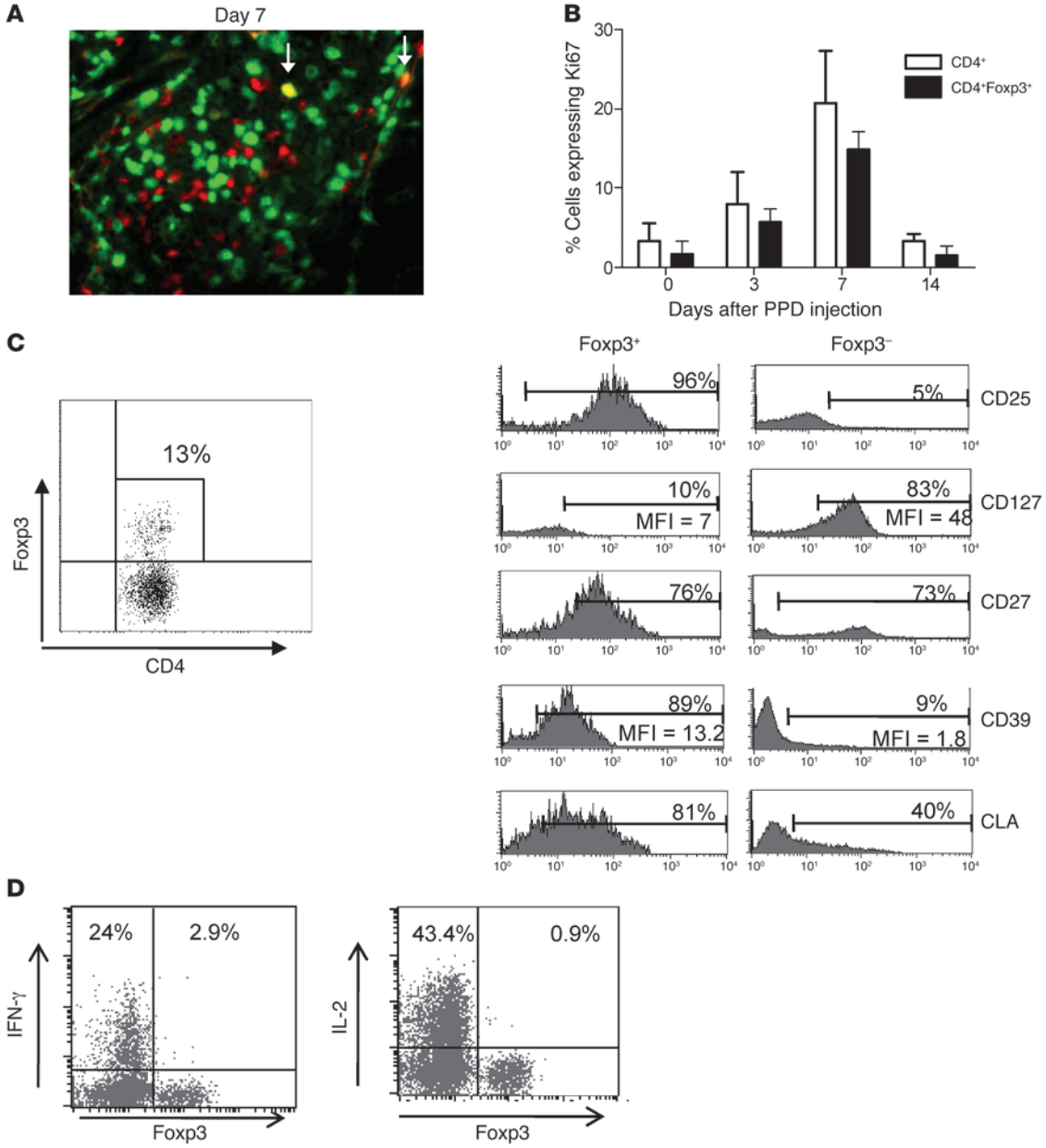

Figure 5

Foxp3+ T cells have a Treg phenotype and proliferate at the site of an immune response. (**A**) Double immunofluorescence staining of Ki67 (green) and Foxp3 (red) in a representative day 7 skin section (original magnification, ×400). Arrows indicate cells staining positive for both Ki67 and Foxp3 (yellow). (**B**) Graph shows the percentage of CD4+ (white bars) and CD4+Foxp3+ (black bars) cells expressing Ki67. Data are mean ± SD; $n = 5$ per time point. (**C**) Blister cells were isolated on day 7 following MT induction and stained for Foxp3, CD127, CD25, CD27, and CD39. Representative staining ($n = 6$) is shown. Dot plot indicates the gating strategy, and histograms show the expression of surface molecules on CD4+Foxp3+ and CD4+Foxp3− subsets. MFI and percentage of positive cells are indicated. CLA, cutaneous lymphocyte antigen. (**D**) Blister cells were isolated on day 7 following MT induction, stimulated with PPD for 15 hours in the presence of brefeldin A, and stained for intracellular expression of cytokines and Foxp3. The percentage of Foxp3+ and Foxp3− cells secreting cytokines is indicated. Dot plots are representative of 4–6 independent experiments.

transiently in T cells is not accompanied by the acquisition of functional characteristics of Tregs, in agreement with previous reports (27, 33, 34).

Foxp3+ T cells at the site of MT proliferate in parallel to effector T cells and have a Treg phenotype. To determine whether the Foxp3+ cells found in the skin represented a Treg population or activated CD4+ T cells that expressed Foxp3 transiently, we double-stained the MT skin sections for Ki67 and Foxp3 expression (Figure 5A). In contrast to the CD4+ T cells that were activated in vitro, where all Foxp3+ cells are also Ki67+, in the skin only a proportion of CD4+Foxp3+ cells expressed Ki67 (14%–33% at all times following PPD injection; mean, 23.2%). The kinetics of Ki67 expression in Foxp3+ (putative Tregs) and CD4+Foxp3− (effector cells) are very similar (Figure 5B). To characterize the Foxp3+ T cells in the skin more extensively, we

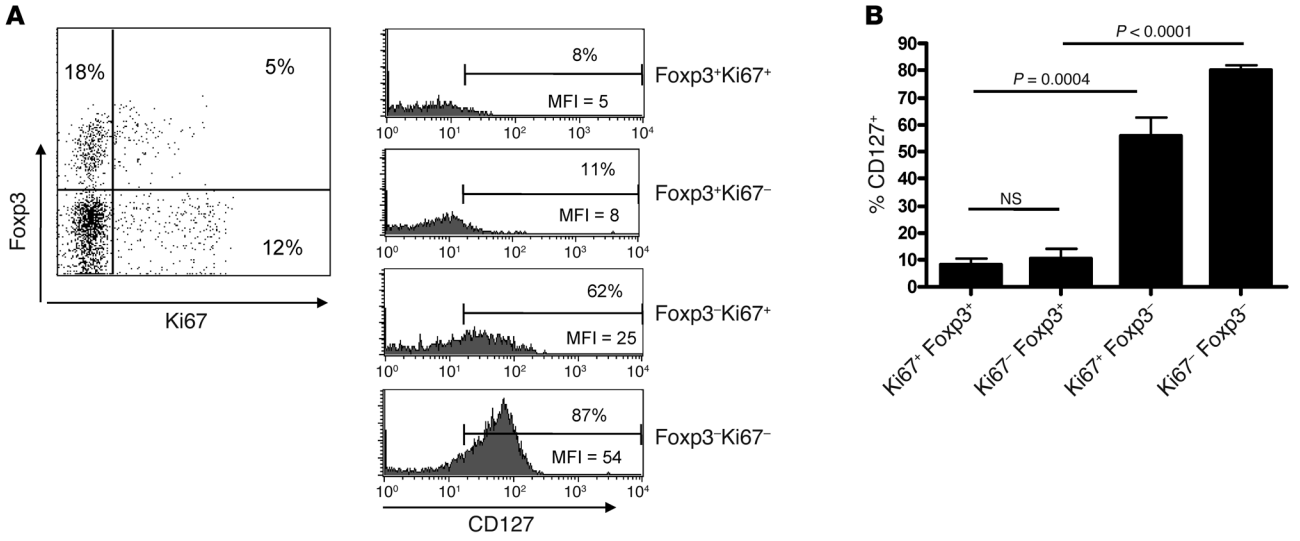

Figure 6

Proliferating Foxp3+ T cells in the skin express low levels of CD127. Blister cells were isolated on day 7 following MT induction and stained for CD4, Foxp3, CD127, and Ki67. Representative staining ($n = 6$) is shown. (**A**) Dot plot indicates gating strategy. The percentage of cells in each quadrant is indicated. Histograms show the expression of CD127 on $CD4^+Foxp3^+$ and $CD4^+Foxp3^-$ subsets divided by Ki67 expression. Numbers indicate the percentage of cells expressing CD127. (**B**) Cumulative data comparing $Foxp3^+Ki67^+$ and $Foxp3^+Ki67^-$ subsets. *P* values were calculated using a paired *t* test. Data are mean ± SEM.

induced skin suction blisters at the site of the MT response on day 7 following PPD injection. This time point was chosen because it coincided with the peak $CD4^+$ T cell infiltration and proliferation. Cells isolated from the blisters were stained for the co-expression of Foxp3 with CD25, CD127, CD39, and CD27, as all these markers have been shown to identify nTregs (19, 35–38) (Figure 5C). The percentage of $Foxp3^+$ cells in day 7 blisters was very similar to that observed in histology (range, 7.1% to 22.2%; mean, 14.5% ± 2.0%; $n = 6$). The majority of Foxp3-expressing $CD4^+$ T cells were $CD25^+$ (78.5% ± 7.5%, $n = 3$) and expressed low levels of CD127 (mean ± SEM, 10% ± 2.7%, $n = 5$). Furthermore, these cells were uniformly $CD27^+$, a hallmark of Tregs at sites of immune activation in vivo (19). Finally, the Foxp3-expressing T cells in skin also express CD39, another marker for nTregs (mean, 83.6% ± 4.0%) (37, 38). In contrast, the $CD4^+Foxp3^-$ T cells that were found in the same samples were largely $CD25^-$ and $CD39^-$ but had high expression of CD127.

Technical limitations, namely very small numbers of leukocytes collected from blisters, precluded purification of the putative Treg population from the skin. For day 7 blisters in 30 subjects that were investigated, a mean of 295,000 cells were obtained (range 40 to 900,000 leukocytes, of which 5%–50% were $CD4^+$ T cells). Therefore, the estimated mean number of $CD4^+CD25^+CD127^{lo}$ cells that were present and that we were unable to isolate with current technology was about 2,000–25,000. However, unlike effector cells, nTregs do not secrete IL-2 and IFN-γ after recent stimulation in vitro (29–32). We therefore investigated the capacity of $Foxp3^+$ and $Foxp3^-$ $CD4^+$ T cells that were isolated from suction blisters to produce effector cytokines following restimulation with antigen in vitro. Cells isolated from day 7 blisters were stimulated with PPD for 16 hours and stained for CD4, Foxp3, and IFN-γ or IL-2. Following restimulation, significantly greater numbers of $CD4^+Foxp3^-$ cells synthesized IFN-γ compared with the $CD4^+Foxp3^+$ T cell population (IFN-γ: $P = 0.015$, Wilcoxon paired test; $n = 6$). Similar data were obtained for IL-2 in 4 separate donors (Figure 5D; $P = 0.06$). Thus, although we were not able to assess suppressive function directly, we found that the $CD4^+Foxp3^+$ cells in the skin after antigenic challenge are not recently activated effector $CD4^+$ T cells and are clearly distinct, phenotypically and functionally, from the $CD4^+Foxp3^-$ population.

Finally, to determine whether the cycling $Foxp3^+$ cells ($Ki67^+$) also exhibit a Treg phenotype, we compared the expression of CD127 on $Foxp3^+Ki67^+$ and $Foxp3^+Ki67^-$ T cells (Figure 6). Both cycling and non-cycling Foxp3-expressing populations expressed low levels of CD127, indicating that they were Tregs (mean ± SEM, 8% ± 2.3% and 10.5% ± 3.2%, respectively; $n = 6$). In contrast, CD127 was highly expressed in both in $Foxp3^-Ki67^+$ and $Foxp3^-Ki67^-$ populations (mean ± SEM, 55.7% ± 7% and 80.1% ± 2%, respectively; $n = 6$). Therefore, we determined that $Foxp3^+$ cells that accumulate during the course of MT have multiple phenotypic and functional characteristics of naturally occurring Tregs, and a significant proportion of these proliferate in parallel with the corresponding effector T cells.

The generation of Tregs from skin-derived memory T cell populations. $Foxp3^+$ Tregs observed during MT could originate from natural $CD4^+CD25^+$ Tregs, which either are resident in the skin or migrate into the skin after immune challenge. Both of these possibilities are supported by observations that some $Foxp3^+$ cells reside in normal human skin (Figure 3B and ref. 25) and that circulating Tregs in humans preferentially express the skin-homing molecules CCR4, CLA (ref. 39 and Supplemental Figure 3), and CCR8 (40). An additional possibility is that some Tregs are derived from memory $CD4^+$ T cells that are activated in the skin after antigenic activation.

To test the possibility that memory $CD4^+$ T cells isolated from the skin can be converted into $CD4^+CD25^{hi}$ Tregs in vitro, we first isolated PPD-specific $CD4^+$ T cells from the skin 21 days after antigen injection, when maximal antigen-specific $CD4^+$ T cells are present (21). Freshly isolated PPD-specific $CD4^+$ T cells from the skin were not anergic and were not suppressive (data not shown).

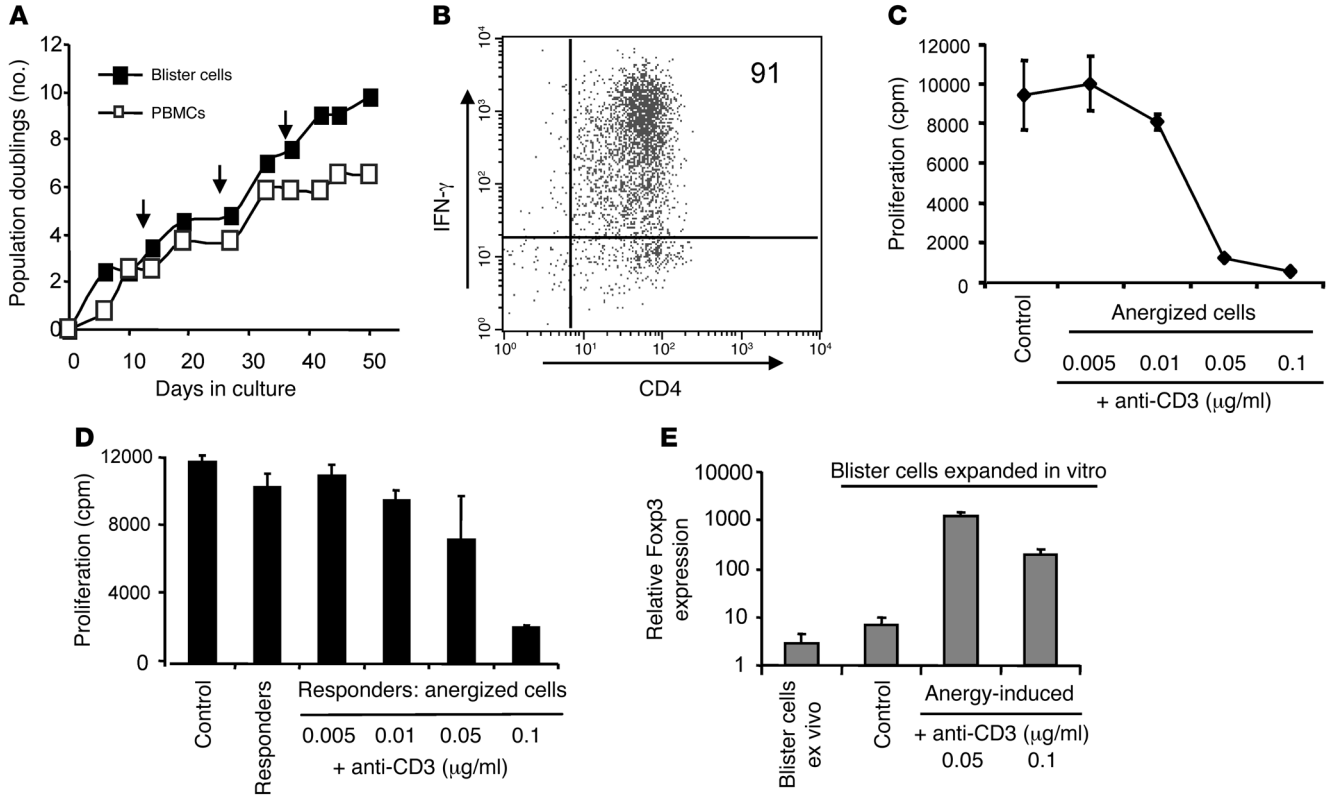

Figure 7

Anergy induction leads to the development of a suppressive phenotype. (**A**) Cells recovered from a suction blister induced over a MT site 21 days following the induction were stimulated in vitro with PPD every 14 days (indicated by arrows). Peripheral blood $CD4^+$ T cells from the same donor were cultured in parallel. (**B**) Dot plot shows IFN-γ production by the cell line in response to PPD stimulation. The percentage of cells expressing IFN-γ is indicated. (**C**) PPD-specific $CD4^+$ T cell line was stimulated with immobilized anti-CD3 mAb. The cells were then washed and stimulated with PPD and antigen-presenting cells for 3 days, and proliferation was measured by $[^3H]$-thymidine incorporation. The mean of triplicate wells ± SEM is shown (representative of 3 separate experiments). PPD-specific $CD4^+$ T cells that were not anergized were used as control. (**D**) Anergized PPD-specific cells described in **C** were mixed with an equal number of autologous non-anergized PPD-specific cells and stimulated with PPD and autologous antigen-presenting cells. Proliferation was measured on day 3 and is expressed as mean ± SEM. Responders, non-anergized PPD cell lines cultured alone; control, responders with non-anergized PPD-specific cells. Results are representative of 2 separate experiments. (**E**) Foxp3 expression was measured by real-time quantitative RT-PCR using 18s rRNA as an internal control. Relative quantity values are plotted in a log-scale bar chart using the triplicate values to estimate SD. Cells recovered from the blister are indicated as "blister cells ex vivo." Blister cells expanded in vitro prior to anergy induction were used as a control.

To obtain sufficient cell numbers for the functional assays, the skin-derived memory T cells were expanded by 3 rounds of stimulation with PPD and autologous irradiated PBMCs in vitro (Figure 7A), after which more than 90% were specific for PPD as determined by IFN-γ production in response to PPD restimulation (Figure 7B). We then investigated whether the expanded PPD-specific CD4 cells could be induced to express Treg markers and acquire suppressive activity. After expansion, PPD-specific $CD4^+$ T cells were still responsive to PPD stimulation (Figure 7, A and B) and did not exhibit suppressive activity (Figure 7D). Previous studies showed that cloned $CD4^+$ T cells could be induced to become regulatory if they were first rendered anergic (41, 42). We therefore anergized these cells by incubating them with immobilized anti-CD3 antibody and found that dose-dependent anergy was induced and that these cells were refractory to subsequent stimulation with PPD and irradiated antigen-presenting cells (Figure 7C and Supplemental Figure 4). In addition, anergized PPD-specific $CD4^+$ T cells suppressed the ability of non-anergized PPD-specific T cell populations to proliferate in response to PPD presented by irradiated autologous antigen-presenting cells (Figure 7D and Supplemental Figure 4). Finally, we showed that, while Foxp3 was expressed at very low levels in both freshly isolated (blister cells ex vivo) and in vitro expanded, non-anergized PPD-stimulated $CD4^+$ T cells derived from the skin (Figure 7E), after anergy induction, there was up to a 100-fold increase in the levels of Foxp3 detected (Figure 7E). In addition, anergized PPD-specific cells show other hallmarks of naturally occurring, $CD4^+CD25^{hi}$ Tregs, including elevated levels of CD25, GITR, and CTLA-4 and low levels CD127 compared with their non-anergized counterparts (data not shown). In separate experiments, an increase in Foxp3 expression following anergy induction was confirmed at the protein level (Supplemental Figure 5). These data indicate that the induction of anergy in activated memory $CD4^+$ T cells isolated from the site of a secondary immune response in vitro can lead to the generation of a Treg population that has all the identical phenotypic and functional characteristics of naturally occurring $CD4^+CD25^{hi}$ Tregs in vivo.

Discussion

The potential for manipulating Tregs for the treatment of T cell–mediated disease is coming closer to reality. A number of therapeutic approaches have been considered, including the expansion of Tregs in vitro followed by reinfusion to treat transplant rejection (43) and also induction of Tregs from responsive T cell populations in vivo with the intention of regulating autoimmunity (reviewed in refs. 11, 16). In addition, depletion of Tregs could be used as a strategy to boost antitumor responses (15). However, there are considerable gaps in our knowledge of the basic biology of human Tregs, including their origin, especially in older adults. Furthermore, the mechanisms that induce their generation from responsive populations of $CD4^+$ T cells remain elusive (17).

We used the MT as a model in order to clarify the balance between Tregs and memory T cells during a secondary immune response in humans because the MT allows sampling of T cells at the site of inflammation (21, 22). Our results indicate that the accumulation of Tregs closely parallels the expansion of $CD4^+$ effector T cells at the site of a controlled immune response. This intimate relationship between both populations suggests that memory T cell proliferation is closely controlled by $CD4^+CD25^{hi}$ Tregs at the peripheral sites of immune reactivity. The origin of the Tregs in the skin is not clear. High expression of skin homing receptors CLA and CCR4 on peripheral blood $Foxp3^+$ cells (39) and on $Foxp3^+$ cells recovered from skin after antigenic challenge suggests that some of the Tregs in the skin may be recruited from the blood (39, 44). Furthermore, we and others (25) have demonstrated that $CD4^+CD25^{hi}Foxp3^+$ Tregs are present in normal skin and it is possible that the increased numbers of these cells at the site of antigenic challenge reflect the proliferation of skin-resident cells. A third, but not mutually exclusive, possibility is that some $CD4^+CD25^{hi}Foxp3^+$ Tregs may be derived from responsive memory $CD4^+$ T cell populations during the immune response in the skin in vivo (17).

In humans, Foxp3 expression does not always correlate with regulatory activity, as it is induced on recently activated $CD4^+$ effector populations (28). Moreover, we show that after activation of nonregulatory $CD4^+Foxp3^-$ T cells in vitro, Foxp3 is transiently expressed by proliferating cells. These recently activated $Foxp3^+$ T cells produce effector cytokines, IL-2, and IFN-γ and are virtually indistinguishable from $CD25^+Foxp3^-$ activated cells in the same cultures (27, 33, 34). The question therefore arises as to whether the $CD4^+Foxp3^+$ T cells that we observed in the skin are actually Tregs or recently activated effector cells. $CD4^+Foxp3^+$ cells isolated from skin blisters expressed all the phenotypic hallmarks associated with natural Tregs ($CD25^{hi}CD39^{hi}CD127^{lo}$) irrespective of whether they were in cell cycle. In contrast $Foxp3^-$ T cells were $CD25^{lo}$ and $CD39^{lo}$, and most were $CD127^{hi}$. Furthermore, previous studies have shown that in inflamed tissues, high expression of CD27 can be used to distinguish Tregs from activated $CD25^+CD4^+$ effectors (19), and we found that $Foxp3^+$ cells isolated from the skin showed uniformly high expression of CD27 (Figure 5C). Finally, $CD4^+Foxp3^+$ cells isolated from skin blisters did not produce any cytokines associated with effector T cells (IL-2, IFN-γ). In contrast, the $CD4^+Foxp3^-$ population synthesized IL-2 and IFN-γ following antigen-specific restimulation in vitro. This is in agreement with the widely accepted view that $Foxp3^+$ Tregs do not produce IL-2 or IFN-γ (29–32). Taken together, these results strongly support the possibility that the $Foxp3^+$ T cells that are found in the skin after secondary antigenic challenge are a Treg population. However, we were not able to assess this directly due to limitations in cell numbers that were obtained from suction blisters.

Populations of memory T cells and Tregs must be maintained in tandem in order to generate controlled immunity, and dysregulation of this balance has been identified in many pathological situations (4, 45). Recent data suggest that the numbers of $CD4^+CD25^{hi}$ Tregs that are present during an immune response may be regulated by proliferation of these cells. In mice, Tregs proliferate substantially in lymphoid tissues (28) as well as in extra-lymphoid sites such as the central nervous system (46), gut lamina propria (12, 20), and skin (47). Although $CD4^+CD25^{hi}$ Tregs in adult humans may originate as a distinct population from the thymus, this organ involutes during aging and is unlikely to be able to totally repopulate the Treg pool in adults (17). It has been shown, however, that $CD4^+CD25^{hi}$ Tregs in healthy adult humans are closely related to and may be derived from the $CD4^+$ memory T cell pool (8, 48, 49). Irrespective of whether human $CD4^+CD25^{hi}$ Tregs are derived from a distinct population from the thymus or from memory T cells in the periphery, they are a highly proliferative population (8). We now extend these observations by showing that their proliferation is coupled to that of memory T cells at the actual site of antigenic challenge in vivo. It would be important to know whether the Treg population also proliferates in the draining lymph node after cutaneous injection of antigen, although this could not be addressed in this study because of obvious ethical constraints.

$CD4^+CD25^{hi}Foxp3^+$ Tregs can be induced from $CD4^+CD25^-Foxp3^-$ T cell populations in vivo and in vitro (17). To assess this in our skin model, we isolated T cells from suction blisters after initiation of the MT and showed that proliferating PPD-specific $CD4^+$ T cells recovered from the site of the immune response in vivo can be converted into functional Tregs through the process of anergy induction in vitro. These anergic cells are phenotypically and functionally indistinguishable from nTregs, suggesting that in principle, a proportion of Tregs in the skin can be derived from the memory T cell pool. Recent studies have described a number of mechanisms, in addition to the induction of anergy, by which Tregs can be generated from responsive T cell populations. Certain cytokines, such as TGF-β, can induce memory $CD4^+$ T cells to become $CD4^+CD25^{hi}Foxp3^+$ Tregs (50), and in some cases, retinoic acid may be involved (51, 52). We are currently investigating the role of TGF-β in the induction of Foxp3 in the skin after antigenic challenge and in the induction of anergy in vitro. Although it is possible that other subsets of Tregs, such as IL-10–secreting Tr1 cells, may also be involved in secondary immune responses, we only detected low levels of this cytokine in suction blisters that were induced at the site of immune challenge (data not shown).

Although clearly possible in vitro, it is not clear whether anergy induction in memory $CD4^+$ T cells also occurs in vivo. Anti-CD3 antibody therapy has been used for the treatment of autoimmunity in mice (53), and clinical trials are in progress to assess the efficacy of this treatment in humans (11). It is thought that one mechanism by which these antibodies may work during treatment is the induction of anergy in effector T cell populations (54). In addition to anti-CD3 treatment, anergy can be induced in responsive T cells by the addition of specific peptides to T cell clones in the absence of antigen-presenting cells (55, 56). In the latter situation, activated human T cell clones, which express high levels of HLA-DR, bind and present the specific peptide to each other, a process known as *T:T presentation* (41). Furthermore a number of studies

support the possibility that T:T presentation may occur in vivo. Degraded peptides generated by enzymatic cleavage of antigens during inflammation can bind to the HLA-DR of the activated T cells (57) or, alternatively, activated T cells might acquire MHC-peptide complexes from antigen-presenting cells (58) or even process and present antigens themselves (59). Furthermore, anergic cells have been shown to persist for extended periods of time in vivo (56, 60) and to exhibit immunoregulatory activity in humans (55), rats (61), and mice (62). The close proximity of activated T cells to each other in the perivascular infiltrates in the skin promotes their interaction with each other to either amplify or inhibit the response. Conversion of conventional $CD4^+$ effector T cells to Foxp3-expressing Tregs is an attractive possibility, as it resolves the problem of limited thymic output and limited expansion capacity of naturally occurring Tregs in humans (8, 17). This possibility is also strengthened by the clonal sharing observed in Treg and effector populations by us and others (8, 48, 49). This, however, does not preclude the derivation of these cells from other sources.

In conclusion, we demonstrate that human $Foxp3^+$ T cells proliferate and accumulate with kinetics very similar to those of memory T cells at the site of a resolving secondary immune response in vivo. Restoring this balance might be of therapeutic benefit in a variety of inflammatory diseases (16, 45). Furthermore, it may be possible to isolate antigen-specific memory cells from sites of inflammation, from which Treg populations may be induced in vitro. The reintroduction of these T cells into the original donors may be a therapeutic strategy for preventing unwanted inflammatory, transplant-related, or autoimmune responses in vivo (63, 64).

Methods

Volunteers. Ethical approval for these studies was obtained from the Ethics Committee of the Royal Free Hospital before recruitment was commenced. A total of 78 young, healthy volunteers with a history of BCG vaccination were recruited. All volunteers provided written informed consent and study procedures were performed in accordance with the principles of the declaration of Helsinki. MT reactions were induced on the flexor aspect of the forearm by the intradermal injection of 0.1 ml of either 10 or 100 U/ml tuberculin PPD (Evans Vaccines Ltd). Induration, palpability, and the change in erythema from baseline were measured and scored on day 3 and at the time of sampling as previously described (21, 22). The MTs were sampled by skin biopsy or skin suction blister at an allotted time point between 0 and 19 days after induction.

Skin suction blisters. Skin suction blister induction involved splitting the epidermis from the dermis by the application of prolonged negative pressure. Suction blisters were raised over MT reactions or normal skin 18–24 hours prior to sampling to ensure maximum cell recovery. A negative pressure of 25–40 kPa (200–300 mmHg) below atmospheric pressure was applied to the skin via a suction chamber for 2–4 hours using a clinical suction pump (VP25, Eschmann) until a unilocular blister measuring 10–15 mm in diameter was formed. A protective dressing was placed over the suction blisters for 18–24 hours, until the blister fluid was aspirated. The blister fluid was microcentrifuged at 650 *g* for 4 minutes to pellet the cellular contents. The pellet was resuspended in complete medium (RPMI; Invitrogen Life Technologies) containing 10% human serum, 100 U/ml penicillin, 100 μg/ml streptomycin, and 2 mM L-glutamine (all from Sigma-Aldrich). Erythrocyte and leukocyte numbers were quantified using a hemocytometer, and viability was assessed by trypan blue exclusion. Skin suction blisters were raised over a total of 63 MT samples at various time points.

PBMC preparation. Heparinized blood was collected from volunteers at the time of blister aspiration. PBMCs were prepared by density centrifugation on Ficoll-Paque (Amersham Biosciences). $CD4^+$ T cells were isolated by negative selection using the VARIO MACS (Miltenyi Biotech). $CD4^+CD25^+$ and $CD4^+CD25^-$ populations were isolated by positive and negative selection, respectively.

Flow cytometric analysis. FACSCalibur (BD) 4-parameter analysis of T cell phenotype was performed as described above. Cells were enumerated after staining with fluorochrome-conjugated CD3 (SK7), CD4 (SK3), and CD8 (SK1) using TruCOUNT tubes (all from BD). Other antibodies used include CD45RA-FITC (L48), IFN-γ–APC (B27), IFN-γ–FITC (25723.11), and IL-2–FITC (5344.111) (all from BD) and CD4-PE (MT310), CD45RA-PE (4KB5), and CD45RB-FITC (PD7/26) (all from Dako). Ki67 staining was performed to identify cells in all stages of cell cycle (23). Ki67-FITC (B56; BD) was used in the intracellular staining protocol (see below). Foxp3 staining was performed using Foxp3-APC (clone PCH101) and the Foxp3 staining kit from eBioscience according to the manufacturer's instructions. In cases in which Ki67 and Foxp3 were used together, the Foxp3 staining protocol was used.

Intracellular cytokine staining. Cells prepared from blisters or peripheral blood were stimulated with 10 μg/ml PPD (Statens Serum Institut) or tetanus toxoid (1:1000 dilution), HSV (concentration), or CMV (1:10) and incubated for 15 hours at 37°C in a humidified 5% CO_2 atmosphere. Brefeldin A (5 μg/ml; Sigma-Aldrich) was added after 2 hours. Unstimulated controls were also included. The cells were then fixed and permeabilized (FIX & PERM Cell Permeabilization Kit; CALTAG Laboratories) before staining for CD3, CD4, IL-2, and IFN-γ. In experiments in which Foxp3 and cytokine staining was performed in parallel, the Foxp3 staining protocol was used according to the manufacturer's instructions.

Foxp3 induction. $CD4^+CD25^-$ T cells were isolated and stained with CFSE (Invitrogen) following the manufacturer's protocol. Cells were then incubated with anti-CD3/CD28–coated T cell expander beads (Dynal; Invitrogen) for up to 7 days, samples were taken at regular intervals,, and the cells were labeled with CD25, Ki67, and Foxp3 (as described above) and acquired on a flow cytometer (FACSCalibur or LSR II; BD Biosciences). For assessment of cytokine secretion by induced $Foxp3^+$ cells, T cells from CD3/CD28-stimulated cultures were collected on day 4 and restimulated with PMA (25 ng/ml) and ionomycin (500 ng/ml), and brefeldin A was added for the last 2 hours of incubation.

Long-term cell culture. Long-term proliferative capacity was assessed by culturing PPD-stimulated PBMCs and blister cells in complete medium supplemented with IL-2 (5 ng/ml). Cells were restimulated with PPD-pulsed (1 μg/ml) autologous irradiated PBMCs every 10–14 days. Fresh medium and IL-2 were added every 3–4 days. Cell numbers and viability were quantified with TruCOUNT tubes. Population doublings (PDs) were calculated using the following equation: PD = log (number of cells counted after expansion) – log (number of cells seeded) / $\log_2$.

Anergy induction and suppression. PPD-specific $CD4^+$ T cell lines were established from blister cells recovered from the site of the MT 19 days after induction (21). Cells for these experiments were harvested after 4 rounds of stimulation with PPD (1 μg/ml) and autologous irradiated PBMCs in vitro (21). Cells (10^6/ml) were incubated in 24-well plates in the presence or absence of increasing concentrations of immobilized anti-CD3 (OKT3) antibody (0.005–0.1 μg/ml) for 18–24 hours at 37°C in a humidified 5% CO_2 atmosphere to induce anergy. Following anergy induction, the cells were washed and stimulated in a 1:1 ratio with autologous irradiated PPD-pulsed (1 μg/ml) PBMCs in 96-well round-bottomed plates to assess anergy induction. Anergized cells were stimulated with an equal number of autologous non-anergized responder PPD cell lines and autologous irradiated PPD-pulsed PBMCs in 96-well round-bottomed

plates to test for suppression. Responder and anergized cells were cultured for 3 days, and [^{3}H]-thymidine was added during the last 16 hours of culture. Proliferative responses were expressed as mean [^{3}H]-thymidine incorporation (cpm) of triplicate wells ± SEM.

Histological analysis of skin biopsies. Skin biopsies were collected at various times after PPD injection (day 0 to day 19). Frozen 5-μm sections of skin biopsies were fixed and stained using indirect immunoperoxidase and double indirect immunofluorescence as previously described (21, 22). When counting the numbers of cells in perivascular infiltrates, the 5 largest perivascular infiltrates present in the upper and middle dermis were selected for analysis. Cell numbers were expressed as the mean absolute cell number counted within the frame (22). Foxp3 staining was performed using a modified protocol of Banham et al. (65). Briefly, the primary antibody (Foxp3-biotin, clone PCH101) was diluted 1:100 in PBS and left to incubate overnight at 4°C. The next day, slides were washed twice in PBS and then incubated with the secondary antibody (streptavidin-Cy3, 1:200; Caltag Laboratories) for 45 minutes at room temperature. Slides were then washed twice in PBS and mounted with Vectashield containing DAPI (Vector Laboratories).

Foxp3 real-time PCR. The primers and probe used were as follows: Foxp3 sense, GAGAAGCTGAGTGCCATGCA; Foxp3 antisense, AGGAGCCCTTGTCGGATGAT; Foxp3 TaqMan probe, AAAATGGCACTGACCAAGGCTTCATCTGT (FAM labeled); 18s rRNA sense, GCCGCTAGAGGTGAAATTCTTG; 18s antisense, CATTCTTGGCAAATGCTTTCG; 18s TaqMan probe, CCGGCGCAAGACGGACCAGA (VIC labeled). All primers and probes were designed using ABI Primer Express version 1.0 (Applied Biosystems). Real-time quantitative RT-PCR was performed on an ABI Prism 7900HT sequence detector (PerkinElmer and Applied Biosystems). For each test sample, 100–200 ng cDNA template was used in a set of triplicate wells. The data were analyzed using SDS 2.2 (Applied Biosystems). CT measurements for 18s rRNA were deducted from Foxp3 CT measurements to calculate the ΔCT. Relative quantity (RQ) values were then calculated ($RQ = 2^{-\Delta CT}$) and plotted in a log-scale bar chart, using the triplicate values to estimate standard deviation.

Statistics. Statistical significance was evaluated using GraphPad software. The Kruskal-Wallis test, 1-way ANOVA, and paired *t* test were used as indicated in the Results and figures. Differences were considered significant at $P < 0.05$.

Acknowledgments

We gratefully acknowledge funding for this work from The British Biological and Biotechnological Science Council, The British Skin Foundation, and The Henry Smith's Charity and Dermatrust. We would like to thank Alison Banham (University of Oxford) for help with establishing the histological analysis of Foxp3 in skin sections and Nigel Klein (Institute of Child Health, University College London) for help with microscopic analysis.

Received for publication April 3, 2008, and accepted in revised form August 20, 2008.

Address correspondence to: Arne N. Akbar, Department of Immunology, UCL Immunology Consortium, 46 Cleveland St., London W1T 4JF, United Kingdom. Phone: (44) 20-76799214; Fax: (44) 20-76799545; E-mail: a.akbar@ucl.ac.uk.

1. Shevach, E.M. 2002. CD4+ CD25+ suppressor T cells: more questions than answers. *Nat. Rev. Immunol.* **2**:389–400.
2. Sakaguchi, S. 2004. Naturally arising CD4+ regulatory t cells for immunologic self-tolerance and negative control of immune responses. *Annu. Rev. Immunol.* **22**:531–562.
3. Coombes, J.L., Robinson, N.J., Maloy, K.J., Uhlig, H.H., and Powrie, F. 2005. Regulatory T cells and intestinal homeostasis. *Immunol.Rev.* **204**:184–194.
4. Belkaid, Y. 2007. Regulatory T cells and infection: a dangerous necessity. *Nat. Rev. Immunol.* **7**:875–888.
5. Apostolou, I., and von Boehmer, H. 2004. In vivo instruction of suppressor commitment in naive T cells. *J. Exp. Med.* **199**:1401–1408.
6. Cobbold, S.P., et al. 2004. Induction of foxP3+ regulatory T cells in the periphery of T cell receptor transgenic mice tolerized to transplants. *J. Immunol.* **172**:6003–6010.
7. Walker, L.S., Chodos, A., Eggena, M., Dooms, H., and Abbas, A.K. 2003. Antigen-dependent proliferation of CD4+ CD25+ regulatory T cells in vivo. *J. Exp. Med.* **198**:249–258.
8. Vukmanovic-Stejic, M., et al. 2006. Human CD4+ CD25hi Foxp3+ regulatory T cells are derived by rapid turnover of memory populations in vivo. *J. Clin. Invest.* **116**:2423–2433.
9. Farzaneh, L., Kasahara, N., and Farzaneh, F. 2007. The strange case of TGN1412. *Cancer Immunol. Immunother.* **56**:129–134.
10. Tarbell, K.V., et al. 2007. Dendritic cell-expanded, islet-specific CD4+ CD25+ CD62L+ regulatory T cells restore normoglycemia in diabetic NOD mice. *J. Exp. Med.* **204**:191–201.
11. Chatenoud, L., and Bluestone, J.A. 2007. CD3-specific antibodies: a portal to the treatment of autoimmunity. *Nat. Rev. Immunol.* **7**:622–632.
12. Mottet, C., Uhlig, H.H., and Powrie, F. 2003. Cutting edge: cure of colitis by CD4+CD25+ regulatory T cells. *J. Immunol.* **170**:3939–3943.
13. Joffre, O., et al. 2008. Prevention of acute and chronic allograft rejection with CD4+CD25+Foxp3+ regulatory T lymphocytes. *Nat. Med.* **14**:88–92.
14. Gregori, S., et al. 2001. Regulatory T cells induced by 1 alpha,25-dihydroxyvitamin D3 and mycophenolate mofetil treatment mediate transplantation tolerance. *J. Immunol.* **167**:1945–1953.
15. Dannull, J., et al. 2005. Enhancement of vaccine-mediated antitumor immunity in cancer patients after depletion of regulatory T cells. *J. Clin. Invest.* **115**:3623–3633.
16. Roncarolo, M.G., and Battaglia, M. 2007. Regulatory T-cell immunotherapy for tolerance to self antigens and alloantigens in humans. *Nat. Rev. Immunol.* **7**:585–598.
17. Akbar, A.N., Vukmanovic-Stejic, M., Taams, L.S., and Macallan, D.C. 2007. The dynamic co-evolution of memory and regulatory CD4+ T cells in the periphery. *Nat. Rev. Immunol.* **7**:231–237.
18. van Amelsfort, J.M., Jacobs, K.M., Bijlsma, J.W., Lafeber, F.P., and Taams, L.S. 2004. CD4(+)CD25(+) regulatory T cells in rheumatoid arthritis: differences in the presence, phenotype, and function between peripheral blood and synovial fluid. *Arthritis Rheum.* **50**:2775–2785.
19. Ruprecht, C.R., et al. 2005. Coexpression of CD25 and CD27 identifies FoxP3+ regulatory T cells in inflamed synovia. *J. Exp. Med.* **201**:1793–1803.
20. Uhlig, H.H., et al. 2006. Characterization of Foxp3+CD4+CD25+ and IL-10-secreting CD4+CD25+ T cells during cure of colitis. *J. Immunol.* **177**:5852–5860.
21. Reed, J.R., et al. 2004. Telomere erosion in memory T cells induced by telomerase inhibition at the site of antigenic challenge in vivo. *J. Exp. Med.* **199**:1433–1443.
22. Orteu, C.H., et al. 1998. The role of apoptosis in the resolution of T cell-mediated cutaneous inflammation. *J. Immunol.* **161**:1619–1629.
23. Gerdes, J., et al. 1984. Cell cycle analysis of a cell proliferation-associated human nuclear antigen defined by the monoclonal antibody Ki-67. *J. Immunol.* **133**:1710–1715.
24. Kalish, R.S., and Johnson, K.L. 1990. Enrichment and function of urushiol (poison ivy)-specific T lymphocytes in lesions of allergic contact dermatitis to urushiol. *J. Immunol.* **145**:3706–3713.
25. Clark, R.A., and Kupper, T.S. 2007. IL-15 and dermal fibroblasts induce proliferation of natural regulatory T cells isolated from human skin. *Blood.* **109**:194–202.
26. Allan, S.E., et al. 2005. The role of 2 FOXP3 isoforms in the generation of human CD4+ Tregs. *J. Clin. Invest.* **115**:3276–3284.
27. Gavin, M.A., et al. 2006. Single-cell analysis of normal and FOXP3-mutant human T cells: FOXP3 expression without regulatory T cell development. *Proc. Natl. Acad. Sci. U. S. A.* **103**:6659–6664.
28. Walker, M.R., Carson, B.D., Nepom, G.T., Ziegler, S.F., and Buckner, J.H. 2005. De novo generation of antigen-specific CD4+CD25+ regulatory T cells from human CD4+CD25- cells. *Proc. Natl. Acad. Sci. U. S. A.* **102**:4103–4108.
29. Pandiyan, P., Zheng, L., Ishihara, S., Reed, J., and Lenardo, M.J. 2007. CD4+CD25+Foxp3+ regulatory T cells induce cytokine deprivation-mediated apoptosis of effector CD4+ T cells. *Nat. Immunol.* **8**:1353–1362.
30. Tiemessen, M.M., et al. 2007. CD4+CD25+Foxp3+ regulatory T cells induce alternative activation of human monocytes/macrophages. *Proc. Natl. Acad. Sci. U. S. A.* **104**:19446–19451.
31. Scott-Browne, J.P., et al. 2007. Expansion and function of Foxp3-expressing T regulatory cells during tuberculosis. *J. Exp. Med.* **204**:2159–2169.
32. Levings, M.K., Sangregorio, R., and Roncarolo, M.G. 2001. Human cd25(+)cd4(+) t regulatory cells suppress naive and memory T cell proliferation and can be expanded in vitro without loss of function. *J. Exp. Med.* **193**:1295–1302.
33. Allan, S.E., et al. 2007. Activation-induced FOXP3 in human T effector cells does not suppress proliferation or cytokine production. *Int. Immunol.* **19**:345–354.
34. Tran, D.Q., Ramsey, H., and Shevach, E.M. 2007. Induction of FOXP3 expression in naive human

CD4+FOXP3 T cells by T-cell receptor stimulation is transforming growth factor-beta dependent but does not confer a regulatory phenotype. *Blood.* **110**:2983–2990.
35. Liu, W., et al. 2006. CD127 expression inversely correlates with FoxP3 and suppressive function of human CD4+ T reg cells. *J. Exp. Med.* **203**:1701–1711.
36. Seddiki, N., et al. 2006. Expression of interleukin (IL)-2 and IL-7 receptors discriminates between human regulatory and activated T cells. *J. Exp. Med.* **203**:1693–1700.
37. Borsellino, G., et al. 2007. Expression of ectonucleotidase CD39 by Foxp3+ Treg cells: hydrolysis of extracellular ATP and immune suppression. *Blood.* **110**:1225–1232.
38. Deaglio, S., et al. 2007. Adenosine generation catalyzed by CD39 and CD73 expressed on regulatory T cells mediates immune suppression. *J. Exp. Med.* **204**:1257–1265.
39. Hirahara, K., et al. 2006. The majority of human peripheral blood CD4+CD25highFoxp3+ regulatory T cells bear functional skin-homing receptors. *J. Immunol.* **177**:4488–4494.
40. Schaerli, P., et al. 2004. A skin-selective homing mechanism for human immune surveillance T cells. *J. Exp. Med.* **199**:1265–1275.
41. Lombardi, G., Sidhu, S., Batchelor, R., and Lechler, R. 1994. Anergic T cells as suppressor cells in vitro. *Science.* **264**:1587–1589.
42. Taams, L.S., et al. 2001. Human anergic/suppressive CD4(+)CD25(+) T cells: a highly differentiated and apoptosis-prone population. *Eur. J. Immunol.* **31**:1122–1131.
43. Hoffmann, P., et al. 2006. Isolation of CD4+CD25+ regulatory T cells for clinical trials. *Biol. Blood Marrow Transplant.* **12**:267–274.
44. Chong, B.F., Murphy, J.E., Kupper, T.S., and Fuhlbrigge, R.C. 2004. E-selectin, thymus- and activation-regulated chemokine/CCL17, and intercellular adhesion molecule-1 are constitutively coexpressed in dermal microvessels: a foundation for a cutaneous immunosurveillance system. *J. Immunol.* **172**:1575–1581.
45. Baecher-Allan, C., and Hafler, D.A. 2006. Human regulatory T cells and their role in autoimmune disease. *Immunol. Rev.* **212**:203–216.
46. Korn, T., et al. 2007. Myelin-specific regulatory T cells accumulate in the CNS but fail to control autoimmune inflammation. *Nat. Med.* **13**:423–431.
47. Suffia, I.J., Reckling, S.K., Piccirillo, C.A., Goldszmid, R.S., and Belkaid, Y. 2006. Infected site-restricted Foxp3+ natural regulatory T cells are specific for microbial antigens. *J. Exp. Med.* **203**:777–788.
48. Kasow, K.A., et al. 2004. Human CD4+CD25+ regulatory T cells share equally complex and comparable repertoires with CD4+. *J. Immunol.* **172**:6123–6128.
49. Scheinberg, P., et al. 2007. The clonal composition of human CD4+CD25+Foxp3+ cells determined by a comprehensive DNA-based multiplex PCR for TCRB gene rearrangements. *J. Immunol. Methods.* **321**:107–120.
50. Fantini, M.C., et al. 2004. Cutting edge: TGF-{beta} induces a regulatory phenotype in CD4+CD25- T cells through Foxp3 induction and down-regulation of Smad7. *J. Immunol.* **172**:5149–5153.
51. Coombes, J.L., et al. 2007. A functionally specialized population of mucosal CD103+ DCs induces Foxp3+ regulatory T cells via a TGF-beta and retinoic acid-dependent mechanism. *J. Exp. Med.* **204**:1757–1764.
52. Sun, C.M., et al. 2007. Small intestine lamina propria dendritic cells promote de novo generation of Foxp3 T reg cells via retinoic acid. *J. Exp. Med.* **204**:1775–1785.
53. Chatenoud, L., Thervet, E., Primo, J., and Bach, J.F. 1994. Anti-CD3 antibody induces long-term remission of overt autoimmunity in nonobese diabetic mice. *Proc. Natl. Acad. Sci. U. S. A.* **91**:123–127.
54. Smith, J.A., Tso, J.Y., Clark, M.R., Cole, M.S., and Bluestone, J.A. 1997. Nonmitogenic anti-CD3 monoclonal antibodies deliver a partial T cell receptor signal and induce clonal anergy. *J. Exp. Med.* **185**:1413–1422.
55. Taams, L.S., et al. 2002. Antigen-specific T cell suppression by human CD4+CD25+ regulatory T cells. *Eur. J. Immunol.* **32**:1621–1630.
56. Lombardi, G., et al. 2000. Type 1 IFN maintains the survival of anergic CD4+ T cells. *J. Immunol.* **165**:3782–3789.
57. LaSalle, J.M., Tolentino, P.J., Freeman, G.J., Nadler, L.M., and Hafler, D.A. 1992. Early signaling defects in human T cells anergized by T cell presentation of autoantigen. *J. Exp. Med.* **176**:177–186.
58. Patel, D.M., et al. 1999. Class II MHC/peptide complexes are released from APC and are acquired by T cell responders during specific antigen recognition. *J. Immunol.* **163**:5201–5210.
59. Barnaba, V., Watts, C., de Boer, M., Lane, P., and Lanzavecchia, A. 1994. Professional presentation of antigen by activated human T cells. *Eur. J. Immunol.* **24**:71–75.
60. Migita, K., and Ochi, A. 1993. The fate of anergic T cells in vivo. *J. Immunol.* **150**:763–770.
61. Taams, L.S., et al. 1998. Anergic T cells actively suppress T cell responses via the antigen-presenting cell. *Eur. J. Immunol.* **28**:2902–2912.
62. Chai, J.G., et al. 1999. Anergic T cells act as suppressor cells in vitro and in vivo. *Eur. J. Immunol.* **29**:686–692.
63. Leen, A.M., et al. 2006. Monoculture-derived T lymphocytes specific for multiple viruses expand and produce clinically relevant effects in immunocompromised individuals. *Nat. Med.* **12**:1160–1166.
64. June, C.H., and Blazar, B.R. 2006. Clinical application of expanded CD4+25+ cells. *Semin. Immunol.* **18**:78–88.
65. Roncador, G., et al. 2005. Analysis of FOXP3 protein expression in human CD4+CD25+ regulatory T cells at the single-cell level. *Eur. J. Immunol.* **35**:1681–1691.